Fnip1 regulates skeletal muscle fiber type specification, fatigue resistance, and susceptibility to muscular dystrophy

Nicholas L. Reyes[a], Glen B. Banks[b], Mark Tsang[a], Daciana Margineantu[c], Haiwei Gu[d], Danijel Djukovic[d], Jacky Chan[a], Michelle Torres[a], H. Denny Liggitt[a], Dinesh K. Hirenallur-S[a], David M. Hockenbery[c], Daniel Raftery[d,e], and Brian M. Iritani[a,1]

[a]The Department of Comparative Medicine, University of Washington, Seattle, WA 98195-7190; [b]Department of Neurology, University of Washington, Seattle, WA 98195; [c]Clinical Division, Fred Hutchinson Cancer Research Center, Seattle, WA 98109-1024; [d]Department of Anesthesiology and Pain Medicine, Mitochondria and Metabolism Center, Northwest Metabolomics Research Center, University of Washington, Seattle, WA 98109-8057; and [e]Public Health Sciences Division, Fred Hutchinson Cancer Research Center, Seattle, WA 98109-1024

Edited* by Robert N. Eisenman, Fred Hutchinson Cancer Research Center, Seattle, WA, and approved December 8, 2014 (received for review July 14, 2014)

Mammalian skeletal muscle is broadly characterized by the presence of two distinct categories of muscle fibers called type I "red" slow twitch and type II "white" fast twitch, which display marked differences in contraction strength, metabolic strategies, and susceptibility to fatigue. The relative representation of each fiber type can have major influences on susceptibility to obesity, diabetes, and muscular dystrophies. However, the molecular factors controlling fiber type specification remain incompletely defined. In this study, we describe the control of fiber type specification and susceptibility to metabolic disease by folliculin interacting protein-1 (Fnip1). Using *Fnip1* null mice, we found that loss of Fnip1 increased the representation of type I fibers characterized by increased myoglobin, slow twitch markers [myosin heavy chain 7 (MyH7), succinate dehydrogenase, troponin I 1, troponin C1, troponin T1], capillary density, and mitochondria number. Cultured *Fnip1*-null muscle fibers had higher oxidative capacity, and isolated *Fnip1*-null skeletal muscles were more resistant to postcontraction fatigue relative to WT skeletal muscles. Biochemical analyses revealed increased activation of the metabolic sensor AMP kinase (AMPK), and increased expression of the AMPK-target and transcriptional coactivator PGC1α in *Fnip1* null skeletal muscle. Genetic disruption of PGC1α rescued normal levels of type I fiber markers MyH7 and myoglobin in *Fnip1*-null mice. Remarkably, loss of Fnip1 profoundly mitigated muscle damage in a murine model of Duchenne muscular dystrophy. These results indicate that Fnip1 controls skeletal muscle fiber type specification and warrant further study to determine whether inhibition of Fnip1 has therapeutic potential in muscular dystrophy diseases.

folliculin | BHD | AMPK | mTOR | PGC1α

Mammalian skeletal muscle is composed of a mosaic of muscle fiber types (type I, type IIa, type IIb, and type IIx), which are categorized based on differences in the abundance of myosin heavy chain (MHC) proteins, mitochondria, and capillary density, strength, fatigue resistance, and metabolic strategies (see ref. 1 for review). Type I "slow twitch" fibers are deep red in color because of high concentrations of myoglobin and high densities of blood capillaries, which support sustained aerobic activity. Type I fibers are also rich in mitochondria, have increased contraction endurance with lesser strength potential, and use predominantly oxidative phosphorylation for energy production. In contrast, type IIb "fast twitch" fibers are pale in color due to low concentrations of myoglobin, contain comparatively low numbers of mitochondria, and rely more heavily on anaerobic glycolysis for energy production. These characteristics allow type II fibers to have considerable strength and contraction speed, but only for short anaerobic bursts of activity before the muscles fatigue. Type IIa/x fibers have hybrid characteristics between type I and type IIb fibers in that they have intermediate numbers of mitochondria and oxidative potential resulting in moderate strength and improved resistance to fatigue. Because slow twitch fibers use predominantly fatty acid oxidation for energy production, increasing the representation of type I fibers provides increased protection against obesity and related metabolic disorders including diabetes (2–5). Hence, identifying molecules that regulate fiber type conversion can profoundly impact susceptibility to metabolic diseases and can influence the pathophysiology of muscular dystrophies.

Over the last decade, studies using transgenic and knockout mice, and chemical agonists and antagonists, have resulted in the identification of several factors that regulate skeletal muscle fiber type differentiation. In particular, the master metabolic sensor AMP kinase (AMPK) has emerged as a key regulator of mitochondrial biogenesis, type I fiber type specification, and endurance adaptations during chronic exercise (6, 7). AMPK is activated in response to metabolic cues such as low energy (high AMP/low ATP), changes in intracellular Ca^{2+}, and exercise (see ref. 8 for review). Upon activation, AMPK helps maintain energy homeostasis by stimulating mitochondrial biogenesis, ATP production, and autophagy, while concurrently inhibiting ATP consumption mediated by mammalian target of rapamycin (mTOR), a major regulator of cell growth and protein synthesis. AMPK regulates muscle metabolism and differentiation by synergizing with Ca^{2+} signaling to modulate expression and stability of the transcriptional regulators peroxisome proliferator-activated receptor-γ coactivator-1α (PGC1α) and PGC1β, which further activate entire genetic

Significance

Folliculin interacting protein-1 (Fnip1) is an intracellular protein known to interact with folliculin (a protein mutated in Birt Hogg Dube' Syndrome) and the master metabolic sensor AMP kinase. However, the roles of Fnip1 in mammalian development and function are unclear. In this study, we used mice deficient in Fnip1 to show that Fnip1 regulates skeletal muscle fiber type specification. Mice deficient in Fnip1 were significantly enriched for highly oxidative skeletal muscle that is more resistant to fatigue than wild-type muscle. Loss of Fnip1 also decreased muscle damage in a mouse model of Duchenne muscular dystrophy. These results reveal a previously unidentified function for Fnip1 and suggest that pharmacological inhibition of Fnip1 may reduce muscle damage in patients with muscular dystrophy.

Author contributions: N.L.R., G.B.B., D.M., H.D.L., D.M.H., D.R., and B.M.I. designed research; N.L.R., G.B.B., M. Tsang, D.M., H.G., D.D., J.C., M. Torres, and D.K.H.-S. performed research; and N.L.R., G.B.B., and B.M.I. wrote the paper.

The authors declare no conflict of interest.

*This Direct Submission article had a prearranged editor.

[1]To whom correspondence should be addressed. Email: biritani@uw.edu.

This article contains supporting information online at www.pnas.org/lookup/suppl/doi:10.1073/pnas.1413021112/-/DCSupplemental.

programs involved in mitochondrial biogenesis, oxidative metabolism, and slow twitch fiber specification (9–12). However, the molecules that link AMPK and PGC1α to fiber type specification are poorly understood.

Through the use of a random ENU mutagenesis strategy in mice to identify novel immune regulatory genes (13), we previously identified a novel mouse pedigree that lacks expression of folliculin interacting protein-1 (Fnip1) due to a 32-bp deletion in the *Fnip1* gene (14). *Fnip1*$^{-/-}$ mice were identified by an absence of B lymphocytes, which was attributed to a block in B-cell development and survival at the pre–B-cell stage. Although the functions of Fnip1 are poorly understood, Fnip1 protein interacts with folliculin, Fnip2 (a related Fnip family member), and all three subunits (α, β, γ) of AMPK (15–17). Mutations in the *Bhd* gene encoding folliculin results in Birt–Hogg–Dube (BHD) Syndrome, a rare human condition characterized by hamartoma formation, pulmonary cysts, and development of renal tumors (18). In the current study, we found that the loss of Fnip1 results in a pronounced shift of skeletal muscle fiber type toward type I slow twitch and type IIa mixed fibers, due in part to increased activation of PGC1α. These results identify a previously unidentified pathway involving Fnip1 in the differentiation of skeletal muscle fiber types and suggest that Fnip1 may be part of a complex linking AMPK with PGC1α.

Results

Loss of Fnip1 Increases the Representation of Type I Skeletal Muscle Fibers. Upon gross observation, skeletal muscle from *Fnip1*$^{-/-}$ mice appeared dark red in coloration compared with wild-type (WT) skeletal muscle (Fig. 1*A* and Fig. S1). Because slow-twitch fibers appear deeper red relative to fast-twitch fibers, we investigated whether loss of Fnip1 alters the composition of skeletal muscle fiber types. We stained sections of gastrocnemius muscles from *Fnip1*$^{-/-}$ and WT mice for enzymes and proteins that are differentially expressed in type I relative to type IIb fibers, including succinate dehydrogenase (SDH; a mitochondrial enzyme involved in oxidative respiration), metachromatic ATPase (pH 4.7) (which allows for differential myofibrillar stain uptake), and slow twitch-specific myosin heavy chain 7 (MYH7). As shown in Fig. 1*B*, WT gastrocnemius (lateral head) muscles consisted of a mixture of SDH^{+} type I and SDH^{-} type IIb fibers. However, *Fnip1*$^{-/-}$ muscle contained almost exclusively SDH^{+} fibers. *Fnip1*$^{-/-}$ muscle also contained an excess of ATPase^{+} (Fig. 1*C*), MyH7^{+} (Fig. 1*D* and Fig. S1), and MyH2^{+} myofibers (Fig. S1) relative to WT muscle. Transmission electron microscopy also revealed increased numbers of subsarcolemmal mitochondria in *Fnip1*$^{-/-}$ muscle relative to WT muscle (Fig. 1*E*). Morphometric analyses with anti-wheat germ agglutinin (WGA) and anti-CD31 (to identify capillaries) showed that *Fnip1*-null muscle fibers are smaller in diameter (Fig. 1*F*) and contain increased numbers of capillaries relative to WT muscle fibers (Fig. 1*G*), which is consistent with increased representation of slow-twitch myofibers.

To further define the apparent shift in muscle fiber types following the loss of Fnip1, we performed quantitative real-time PCR (qPCR) and immunoblotting to determine the abundance of mRNA and proteins characteristic of type I versus type IIb myofibers. qPCR revealed an ~threefold increase in *Myoglobin* mRNA expression in *Fnip1*$^{-/-}$ skeletal muscle compared with controls, and pronounced increases in mRNA expression of cytoskeletal markers of slow twitch muscle including *Troponin I* slow (*Tnni1*), *Tnnc1*, *Tnnt1*, and *MyH7* (Fig. 2*A*), with corresponding decreases in the transcript levels of MyH4, which is a marker of type IIb fast-twitch fibers (Fig. 2*B*). Immunoblot analyses confirmed significant increases in Myoglobin, MyH7, and cytochrome C proteins in *Fnip1* null gastrocnemius muscle compared with WT muscle (Fig. 2*C*).

Because increased activity could theoretically result in increased oxidative fibers in *Fnip1*$^{-/-}$ mice, we measured ambulatory activity levels in *Fnip1*$^{-/-}$ versus *Fnip1*$^{+/-}$ mice. We found no significant difference in activity levels during either the light or dark cycles (Fig. S2). These results collectively suggest that loss of Fnip1 results in a significant shift in the representation of skeletal muscle fibers from fast twitch type IIb to slow twitch type I and mixed type IIa fibers.

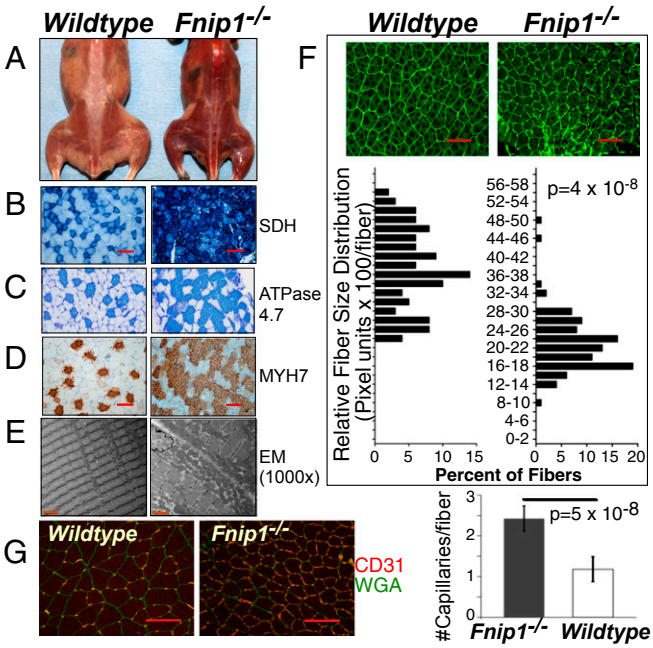

Fig. 1. Fnip1 null skeletal muscle is characterized by deep red coloration; increased SDH, ATPase pH 4.7, and MyH7 staining; increased mitochondria, decreased myofibril size, and increased capillary density indicative of slow twitch skeletal muscle. (*A*) Representative photographs showing WT and *Fnip1*$^{-/-}$ skeletal muscle after euthanasia. (*B–D*) Immunohistochemistry staining of mitochondrial and slow twitch myofiber markers was performed on cross-sections of the lateral head, gastrocnemius muscle. Shown are representative SDH (*B*); ATPase (pH 4.7) (*C*); and myosin heavy chain 7 (MyH7) (*D*) stained sections from $n = 3–5$ 8-wk-old mice per group. (*E*) Increased mitochondria in *Fnip1*$^{-/-}$ muscle. Electron micrographs of the gastrocnemius muscle taken from 8-wk-old male mice. Shown are representative 1,000× images. (*F*) Representative wheat germ agglutinin (WGA) stained cross-sections of WT and *Fnip1* null gastrocnemius muscles. Images were analyzed by fluorescence microscopy, and cross-sectional area was measured. Bar graphs depict relative fiber size distribution of a total of 100 individual fibers per genotype ($n = 3$ mice per group). Wt mean = 3,929 (pixels per fiber), *Fnip1*$^{-/-}$ mean = 2,199 (pixels per fiber); *P* values shown. (*G*) Increased capillary density in *Fnip1*$^{-/-}$ relative to WT gastrocnemius muscle. Sections from 8- to 12-wk-old mice were stained with WGA and anti-CD31. Shown are representative immunofluorescence photos. Graphs represent the mean and SEM of four *Fnip1*$^{-/-}$ and 4 *Fnip1*$^{+/-}$ gastrocnemius muscles. *P* values are shown. (Scale bars: *B*, *D*, and *G*, 100 μm; *E*, 2 μm.)

***Fnip1* Null Skeletal Muscle Contains Increased Numbers of Highly Functional Mitochondria.** To further define the role of Fnip1 in fiber type specification, we assessed the normal levels of Fnip1 protein in muscles with type IIb characteristics [extensor digitalis longus (EDL) and gastrocnemius] versus type I characteristics (Soleus). We found that in WT skeletal muscles, Fnip1 protein is expressed in muscles rich in type IIb fibers (EDL, gastrocnemius), but is low or absent in soleus muscles, which are rich in type I fibers (Fig. S3). These results are consistent with the notion that Fnip1 has a role in fiber type specification. To characterize the consequences of Fnip1 loss on the metabolic capacity of muscle fibers, we assessed levels of key mitochondrial gene transcripts and measured the metabolic capacity of myofibrils from *Fnip1*$^{-/-}$ and WT gastrocnemius muscle. qPCR analysis indicated that relative to WT muscle, disruption of Fnip1 resulted in increased levels of mitochondrial gene transcripts including

DEVELOPMENTAL BIOLOGY

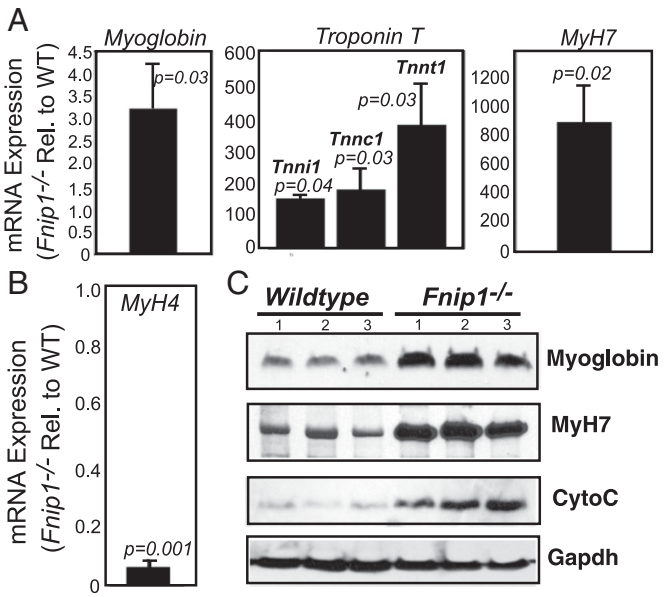

Fig. 2. Fnip1 null skeletal muscle expresses increased levels of slow twitch-specific genes and proteins. (*A* and *B*) Gastrocnemius muscle RNA was extracted from 8-wk-old male mice. Gene expression was measured by qPCR. Shown are the means ± SEM from 4 to 6 mice per group. mRNA expression levels are shown as *Fnip1*$^{-/-}$ relative to WT mice. (*C*) Immunoblotting of proteins characteristic of slow twitch muscle fibers. Proteins were isolated from gastrocnemius muscle. Shown are representative immunoblots showing three independent mice per group. Gapdh is shown as loading controls. *P* values are shown (Student's *t* test).

cytochrome B (*Cytb*), ATP synthase lipid binding protein (*Atp5γ1*), and uncoupling protein 3 (*Ucp3*) (Fig. S3).

To assess the functional consequences of the increased mitochondria mass in *Fnip1*$^{-/-}$ skeletal muscle, we isolated adult myofibers from *Fnip1*$^{-/-}$ and WT mice and assessed basal bioenergetic metabolism by using the Seahorse XF analyzer, which measures oxygen consumption rate (OCR; a measure of oxidative phosphorylation) on live cultured cells. We found that *Fnip1*$^{-/-}$ myofibrils exhibit significantly increased basal OCR relative to WT myofibrils (Fig. S3), suggesting that disruption of *Fnip1* results in a pronounced expansion of functional mitochondria.

To better define this observed metabolic shift, we performed targeted metabolomics using liquid chromatography tandem mass spectrometry (LC-MS/MS) to measure alterations in levels of 158 metabolites associated with major metabolic pathways. We found that *Fnip1*$^{-/-}$ gastrocnemius muscle contained increased metabolites associated with amino acid signaling (glutamine, asparagine, and glutamic acid), and progression of the TCA cycle (α-ketoglutaric acid, aconitate), consistent with increased mTOR signaling (further discussed below) and increased oxidative metabolism (Table S1). Collectively, our results are consistent with a normal role for Fnip1 in the generation and/or maintenance of type IIb fibers, and a shift to oxidative type I and IIa fibers following disruption of *Fnip1*.

Increased Activation of AMPK and PGC1α in Fnip1 Null Skeletal Muscle. Because Fnip1 directly interacts with AMPK, we compared RNA and protein levels of components of the AMPK signaling pathway in gastrocnemius muscle from *Fnip1*$^{-/-}$ and WT mice. Levels of phosphorylated AMPK and phosphorylated acetyl CoA carboxylase 1 (ACC1) were increased in *Fnip1*$^{-/-}$ skeletal muscle relative to WT muscle, which is indicative of activated AMPK (Fig. 3*A*). Expression of the AMPK target and transcriptional coactivator PGC1α was significantly elevated at both the protein (Fig. 3*A*) and mRNA (Fig. 3*B*) level in skeletal muscle from *Fnip1*$^{-/-}$ relative to WT mice (19, 20). Transcript levels of *Pparα*, *Pparδ*, and *PGC1β* (coactivation targets of PGC1α) (6) were also increased in *Fnip1*$^{-/-}$ mice. These results collectively suggest that disruption of *Fnip1* results in increased basal activation of AMPK, which targets multiple transcriptional programs controlled by its substrates including PGC1α (6).

Increased mTORC1 Activity in *Fnip1* Null Skeletal Muscle. Mammalian target of rapamycin consists of the rapamycin-sensitive mTORC1 complex (mTOR, Raptor, Pras-40, Deptor, mLST8) and the rapamycin-insensitive mTORC2 complex (mTOR, Rictor, mSin1, Protor, Deptor, and mLST8) (21). mTORC1 promotes cell growth by inducing protein synthesis and cell cycle progression in response to amino acids and growth factors. In contrast, mTORC2 regulates cell survival and cytoskeletal organization in response to growth factors. Under energy-deficient conditions, activated AMPK inhibits energy consuming cellular growth driven by the mTORC1 pathway in part by phosphorylating and activating the mTORC1 inhibitor TSC2, and by phosphorylating and inhibiting the mTORC1-activating adaptor Raptor (8). Because mTORC1 has been shown to enhance mitochondrial biogenesis in skeletal muscle, we sought to determine whether mTORC1 is regulated by Fnip1. Immunoblot analysis revealed increased phosphorylation of ribosomal S6 protein (S6R) and EIF4E-binding protein 1 (P-4EBP1) in *Fnip1*$^{-/-}$ gastrocnemius muscle relative to WT muscle (Fig. S4). P-S6R and P-4EBP are downstream products of mTORC1 activation and are commonly used as markers of mTORC1 activity. mTORC1 is also regulated by a negative-feedback loop resulting in reduced expression of growth factor receptors and decreased PI3K signaling (21). Indeed, we found a reduction of biphosphorylated glycogen synthase kinase-3 (GSK-3) which is phosphorylated by protein kinase B (AKT), a downstream effecter of PI3 kinase (Fig. S4). Inhibition of GSK activation is likely a consequence of mTORC1 self-regulation through inhibition of PI3-kinase and subsequently AKT.

We next examined whether hyperactive mTOR might be responsible for the shift in skeletal muscle fiber type following disruption of *Fnip1*. We treated *Fnip1*$^{-/-}$ mice with the mTORC1 inhibitor rapamycin beginning at conception (i.e., breeding pairs were treated with rapamycin diet) through weaning until 6 wk of age when gastrocnemius muscles were harvested and analyzed. We found that long-term rapamycin treatment failed to reduce levels of the slow twitch markers MyH7, myoglobin, and PGC1α in *Fnip1*$^{-/-}$ mice relative to WT mice despite inhibition mTORC1 activity (pS6R) to below basal WT levels (Fig. S4). These results collectively support a role of Fnip1 in skeletal muscle fiber type representation relatively independent of mTORC1.

Fnip1 Null Skeletal Muscle Is More Resistant to Fatigue. To investigate the functional significance of the shift in fiber type following

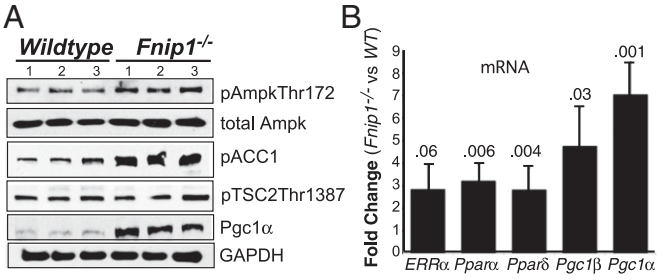

Fig. 3. *Fnip1*$^{-/-}$ skeletal muscles exhibit hyperactivation of the AMPK/PGC1α pathway. (*A*) Immunoblots were performed on protein lysate extracted from gastrocnemius muscles of age- and sex-matched mice. Shown are representative immunoblots from five mice of each genotype. Numbers 1, 2, and 3 represent individual mice of each genotype. (*B*) Expression of *ERRα*, *Pparα*, *Pparδ*, *PGC1α*, and *PGC1β* were determined via qPCR on RNA extracted from the gastrocnemius of age- and sex-matched mice. Shown are bar graphs depicting the mean ± SEM from six mice per group.

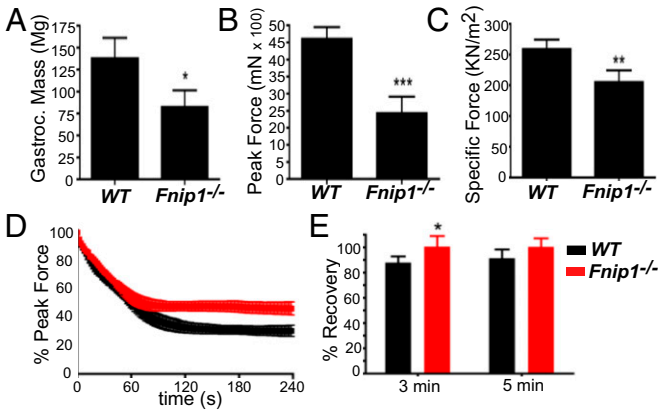

Fig. 4. *Fnip1* null skeletal muscles are more resistant to fatigue and have more rapid postcontraction recovery. (*A*) Reduced mass of gastrocnemius muscle isolated from *Fnip1*$^{-/-}$ mice relative to WT mice. Shown is the mean ± SEM from four mice per group. (*B* and *C*) *Fnip1*$^{-/-}$ mice produce reduced specific force (*B*) and peak force (*C*) relative to WT mice. Contraction force measurements were performed in situ on gastrocnemius muscle from anesthetized 8-wk-old male *Fnip1*$^{-/-}$ and WT mice in situ. $n = 4$ mice per group. (*D*) *Fnip1*$^{-/-}$ mice exhibit decreased postcontraction refractory duration relative to WT mice. The isolated muscle was stimulated to contract every 2 s for a total of 4 min. Subsequent to repeated contraction muscle was allowed to rest for a period of 3 min, directly followed by a single stimulation and measurement of the resulting recovery force. Red bar, *Fnip1*$^{-/-}$ ($n = 4$); black bar, WT control ($n = 4$). This protocol was repeated at an interval of 5 min. (*E*) Improved percent postcontraction recovery following disruption of Fnip1. Shown are the mean and SEM from 4 mice per group. *$P < 0.05$; **$P < 0.01$; ***$P < 0.005$ (Student's *t* test).

disruption of Fnip1, we performed an in situ muscle fatigue assay to evaluate contraction characteristics of single isolated gastrocnemius muscle bellies from anesthetized *Fnip1*$^{-/-}$ and WT mice. We found that intact *Fnip1*$^{-/-}$ muscles were smaller than that of the WT controls (Fig. 4*A* and Fig. S1). *Fnip1*$^{-/-}$ muscles produced significantly reduced peak force and specific force capacity compared with WT mice (Fig. 4 *B* and *C*). Following repeated stimulation, contraction forces dropped progressively in both WT and *Fnip1*$^{-/-}$ mice, reaching trough force levels after 60 s (Fig. 4*D*). However, whereas *Fnip1*$^{-/-}$ mice plateaued at ∼50% of peak force, WT mice dropped much further to ∼30% of peak force (Fig. 4*D*). Following repeated contraction, *Fnip1* null mice recovered significantly faster than WT controls, returning to 100% of baseline peak force within 3 min after contraction (Fig. 4*E*), whereas WT gastrocnemius muscles remained at ∼85% peak force. The reduction in muscle size, increased endurance, and resistance to fatigue following disruption of *Fnip1* are consistent with a shift in fiber type ratio toward highly oxidative slow twitch fibers.

Loss of Fnip1 Stimulates Type I Fiber Type Differentiation in a PGC1α-Dependent Manner. PGC1α is a key driver of metabolic reprogramming, mitochondrial biogenesis, and type I oxidative fiber specification in skeletal muscle. Because disruption of *Fnip1* results in increased expression of PGC1α (Fig. 3), we sought to determine whether the muscle fiber shift observed in *Fnip1*$^{-/-}$ mice is due in part to the induction of PGC1α. We bred *Fnip1*$^{-/-}$ mice with *PGC1α* null mice (22) to generate *Fnip1*$^{-/-}$ *PGC1α*$^{-/-}$ double-null mice. Upon gross examination, disruption of *PGC1α* partially restored normal coloration of *Fnip1*$^{-/-}$ skeletal muscle (Fig. 5*A*). Immunoblot analysis of gastrocnemius muscle revealed a pronounced reduction in MyH7, cytochrome C, and total myoglobin in *Fnip1*$^{-/-}$ *PGC1α*$^{-/-}$ mice compared with *Fnip1*$^{-/-}$ mice (Fig. 5*B*), suggesting a significant reduction in the representation of slow twitch fibers. These findings identify *PGC1a* as an essential mediator of the oxidative muscle fiber shift seen in *Fnip1* null mice.

Disruption of Fnip1 Mitigates Muscular Dystrophy in a Murine Model of Duchenne Muscular Dystrophy. Duchenne muscular dystrophy (DMD) is a fatal recessive X-linked hereditary disease characterized by progressive muscular dystrophy, which ultimately leads to paralysis and death from respiratory and/or cardiac failure (23). DMD is caused by mutations in the *DMD* gene encoding dystrophin (24–26), a subsarcolemmal protein that functions as part of the dystrophin-associated glycoprotein complex (DGC). Disruption of the DGC in DMD leads to mitochondrial dysfunction, sarcolemmal ruptures, muscle necrosis, and irreversible muscle wasting. Because *Fnip1*$^{-/-}$ skeletal muscle contains increased numbers of functional mitochondria, we determined whether disruption of *Fnip1* could ameliorate the dystrophic pathology in DMD. We bred *Fnip1*$^{-/-}$ mice to *Dmd*$^{mdx\text{-}4CV}$ (*mdx4CV*) mice (27), which have a nonsense codon in exon 53 resulting in the absence of dystrophin protein (28). To examine the effects of *Fnip1* loss on muscle morphology in *mdx4CV* mice, we stained cross-sections of WT, *Fnip1*$^{-/-}$, *mdx4CV*, and *Fnip1*$^{-/-}$ *mdx4CV* gastrocnemius muscle with hematoxylin and eosin, and anti-WGA combined with DAPI, to better visualize the sarcolemma and nuclei. We found that muscle fibers from *mdx4CV* mice have increased numbers of centralized nuclei, which reflects fiber regeneration following muscle injury (Fig. 6*A* and Fig. S5). Concurrent disruption of *Fnip1* in *mdx4CV* mice led to a ∼50% reduction in the percentage of centrally located nuclei. Disruption of *Fnip1* also prevented extravasation of Evans blue dye (EBD) 20 h after i.v. injection (Fig. 6*B* and Fig. S5). EBD extravasation is a common measure of increased vascular and cellular permeability that occurs following muscle damage. To further assess the potential benefits of *Fnip1* loss on inhibiting muscle damage in *mdx4CV* mice, we measured levels of serum creatine kinase (CK), which is a sensitive measure of muscle damage. As expected, *mdx4CV* mice had a ∼14-fold mean increase in levels of CK relative to WT mice (Fig. 6*C*). Remarkably, disruption of *Fnip1* profoundly reduced CK levels in *Fnip1*$^{-/-}$*mdx4CV* mice to levels similar to that of WT mice. Prevention of muscle damage was not likely due to compensatory up-regulation of the dystrophin homolog utrophin, which was reduced in *Fnip1*$^{-/-}$*mdx4CV* mice relative to *mdx4CV* mice (Fig. 6*D* and Fig. S5). These results indicate that inhibition of Fnip1 provides

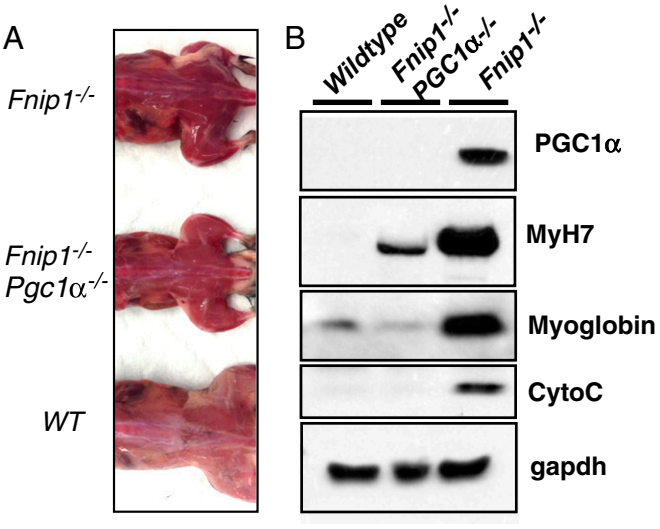

Fig. 5. Disruption of PGC1α reduces levels of oxidative type 1 fiber markers in *Fnip1* null mice. (*A*) *Fnip1*$^{-/-}$*PGC1α*$^{-/-}$ double null mice display an intermediate skeletal muscle coloration phenotype relative to WT and *Fnip1*$^{-/-}$ mice. Shown is a representative photograph from 4 mice per group. (*B*) Immunoblots were performed on protein lysate extracted from the gastrocnemius muscles of age- and sex-matched mice. Note reduction in MyH7, Myoglobin, and cytochrome C proteins in *Fnip1*$^{-/-}$*Pgc1α*$^{-/-}$ versus *Fnip1*$^{-/-}$ mice.

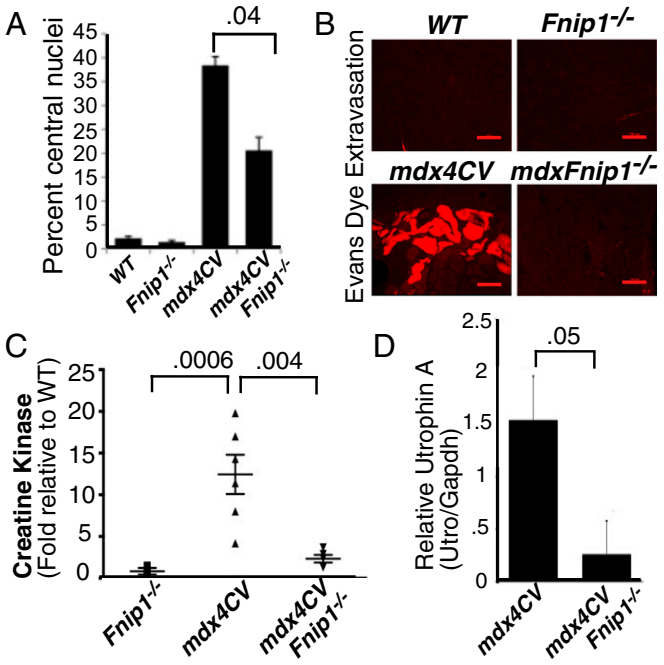

Fig. 6. Disruption of Fnip1 significantly reduces muscle fiber damage and restores muscle fiber integrity in muscular dystrophy mice. *Fnip1*$^{-/-}$ mice were bred to *mdx4CV* mice to generate mice of the indicated genotypes. (*A*) Quadriceps muscles were stained with hematoxylin and eosin (H and E), and wheat germ agglutinin plus DAPI, which assists in visualizing plasma membranes and nuclei. Nuclei were counted in 10 random fields per genotype (n = 3 per genotype) in a blinded fashion. (*B*) Loss of *Fnip1* expression significantly reduces extravasation of EBD in *mdx4CV* mice. Shown are representative images of cross-sections of gastrocnemius muscle harvested from mice of the listed genotypes. Dye leakage was analyzed by fluorescent microscopy. (*C*) Inhibition of Fnip1 significantly reduces serum creatine kinase levels in *mdx4CV* mice. Creatine kinase levels were determined by colorimetric assay. n = 5–6 mice per group. (*D*) Utrophin protein expression in decreased in *Fnip1*$^{-/-}$ mice. Protein was extracted from quadricepts muscle, and utrophin was measured by immunoblotting. Bar graphs represent the mean ± SEM of three mice per genotype. *P* values are shown (Student's *t* test).

significant protection against muscle damage in the *mdx4CV* model of Duchenne muscular dystrophy.

Discussion

The benefits of endurance exercise on skeletal muscle function and resistance to obesity occur in part through the metabolic reprogramming of myofibers, which results in increased utilization of fatty acids, improved resistance to fatigue, and increased protection against obesity and metabolic diseases including diabetes and cardiovascular disease (2–5). In this study, we found that disruption of *Fnip1* results in a shift in skeletal muscle fiber type from predominantly type IIb glycolytic fibers to type I and type IIa oxidative fibers that are rich in mitochondria and capillaries and preferentially use oxidative phosphorylation over glycolysis. Our results identify Fnip1 as an integral member of a signaling pathway involved in programming skeletal muscle fiber specification, and suggest that inhibition of Fnip1 has "exercise mimetic" properties, which has potential to profoundly impact overall metabolic health.

How might Fnip1 regulate fiber type specification? AMPK is hyperactivated in *Fnip1* null muscle based on increased phosphorylation of AMPK at Thr172, and increased phosphorylation of ACC1, an AMPK target involved in lipid metabolism. AMPK was shown to be a major signaling molecule involved in specifying skeletal muscle fiber type differentiation and mitochondrial biogenesis (29) in response to endurance exercise and chronic energy deprivation. For example, gain-of-function mutations in the AMPK γ3 subunit in mice increased mitochondrial biogenesis and oxidative potential in glycolytic skeletal muscle, and provided protection from dietary-induced insulin resistance (30). Similarly, exercise training and the AMPK agonist AICAR increased oxidative fibers, running endurance, and glucose uptake in adult mice (6, 31). Conversely, reduced AMPK activity in AMPKα2 (32, 33) or AMPK β1β2 null mice (34) lead to decreased skeletal muscle mitochondrial function and increased insulin resistance (31, 35). Thus, our results are consistent with Fnip1 regulating mitochondrial biogenesis and fiber type determination in part by directly or indirectly regulating AMPK. Because our study was performed by whole body deletion of *Fnip1*, we cannot discern whether the shift in skeletal muscle fiber type is autonomous to muscle cells. However, activity levels were not increased in *Fnip1*$^{-/-}$ mice, suggesting that increased activity is not causing the shift in fiber representation.

To further define the mechanism whereby Fnip1 regulates mitochondrial biogenesis and fiber type determination, we assessed levels of PGC1α, a master transcriptional coactivator known to regulate these processes downstream of AMPK. PGC1α, and the related PCG1β, have been shown to initiate a program of mitochondrial biogenesis and oxidative phosphorylation by increasing transcription of components of the electron transport chain, TCA cycle, and fatty acid oxidation (36). PGC1α is preferentially expressed in "red" oxidative fibers, and transgenic expression of PGC1α (4) or PCG1β (5) in skeletal muscle fibers increases mitochondrial content, cellular respiration, and fatigue resistance. In our study, we found that disruption of *Fnip1* results in increased levels of PGC1α transcripts and protein. Genetic disruption of *PGC1α* significantly reduced expression of the slow-twitch specific MyH7, myoglobin, and cytochrome C in *PGC1α*$^{-/-}$*Fnip1*$^{-/-}$ relative to *Fnip1*$^{-/-}$ gastrocnemius muscles. These results demonstrate that disruption of *Fnip1* results in increased levels of PGC1α protein, which, in turn, contributes to increased mitochondrial biogenesis and muscle fiber type switch.

It is not clear how loss of Fnip1 results in increased PGC1α. Fnip1 physically interacts with folliculin, Fnip2, HSP90, and all three subunits of AMPK. AMPK stimulates mitochondria biogenesis and increases oxidative phosphorylation resulting in ATP production, in part by increasing expression of *PGC1α* and by phosphorylating PGC1α (20), resulting in increased protein stabilization. Other studies have shown that AMPK phosphorylates both Fnip1 and folliculin (15), and inhibition of folliculin in mice also induces mitochondrial biogenesis and skeletal muscle fiber type switch in a PGC1α-dependent manner (37). Hence, the complex of Fnip1 and folliculin may function in a negative feedback loop to inhibit or "turn off" AMPK, PGC1α, and oxidative metabolism following AMPK activation (Fig. S6). In the absence of Fnip1 or folliculin, AMPK is hyperactivated, resulting in increased PGC1α expression and oxidative metabolism. Consistent with this notion, a recent study concluded that folliculin represses AMPK activation and PGC1α up-regulation in primary mouse embryonic fibroblasts (38), and a separate study concluded that folliculin represses AMPK in *Caenorhabditis elegans* (39), although mechanism(s) for repression were not determined in either study. However, whereas loss of Fnip1 mimics many aspects of AMPK activation in skeletal muscle, there are also important differences. For example, others have shown that activated AMPK inhibits cell growth by inhibiting mTOR. We found that both AMPK and mTOR are hyperactivated in *Fnip1*$^{-/-}$ skeletal muscle, pre-B cells, and iNKT cells (40), suggesting that Fnip1 could have several functions including "turning off" AMPK following activation and coupling AMPK to mTOR inhibition.

Muscular dystrophy diseases are often typified by defective mitochondria (41), and slow oxidative fibers have been shown to be more resistant to dystrophic pathology than fast, glycolytic fibers (42). In this study, we found that inhibition of Fnip1 attenuates severe dystrophic pathology in the *mdx4CV* murine model of DMD (43). Overexpression of PGC1α specifically in skeletal muscle also protects against muscle dystrophy (44),

suggesting that inhibition of Fnip1 may act in part through induction of PGC1α. Given the role of Fnip1 in skeletal muscle fiber type differentiation, capillary density, mitochondrial biogenesis, and resistance to fatigue, these results warrant further investigation as to whether pharmacological inhibition of Fnip1 may provide an innovative strategy to improve muscle function on patients with muscular dystrophy diseases and/or improve the responses of patients with obesity-associated disease.

Materials and Methods

Transgenic Animals. *Fnip1*$^{-/-}$ mice were developed as described (14). The majority of the studies were performed on 8- to 12-wk-old male mice. *PGC1*α (22) and *Dmd*^{Mdx4CV} (27) mice were obtained from Jackson Laboratories and the Chamberlain laboratory, respectively. Mice were housed under specific pathogen-free conditions. Animal studies were reviewed and approved by the Institutional Care and Use Committee of the University of Washington.

Immunohistochemistry and Metachromatic ATPase Staining. Gastrocnemius muscles were collected and were flash frozen in OCT before sectioning. All special staining was performed at the Histology and Imaging Core. High power immunohistochemistry images were performed on the lateral head after removal of the soleus muscle. MyH7 antibody was obtained from Sigma-Aldrich.

Serum Creatine Kinase Assay. Creatine kinase was measured in serum according to manufacturer's instructions [Creatinine Kinase-SL Reagent Kit (Sekisui Diagnostics P.E.I. Inc.)].

EBD Assay. A 1% solution of EBD was injected i.p. at a volume dose of 1% of body weight. Approximately 20 h following injection, mice were killed and the gastrocnemius muscles were snap frozen in OCT media. Leakage of EBD was analyzed by fluorescence microscopy (44).

ACKNOWLEDGMENTS. We thank the Ruddell laboratory for assistance with the fluorescent microscopy. This study was supported by NIH Grants K26RR024462, R56AI092093, P30-DK035816, and R25RR032027 (to B.M.I.).

1. Schiaffino S, Reggiani C (2011) Fiber types in mammalian skeletal muscles. *Physiol Rev* 91(4):1447–1531.
2. Stuart CA, et al. (2013) Slow-twitch fiber proportion in skeletal muscle correlates with insulin responsiveness. *J Clin Endocrinol Metab* 98(5):2027–2036.
3. Hambrecht R, et al. (1997) Effects of endurance training on mitochondrial ultrastructure and fiber type distribution in skeletal muscle of patients with stable chronic heart failure. *J Am Coll Cardiol* 29(5):1067–1073.
4. Lin J, et al. (2002) Transcriptional co-activator PGC-1 alpha drives the formation of slow-twitch muscle fibres. *Nature* 418(6899):797–801.
5. Arany Z, et al. (2007) The transcriptional coactivator PGC-1beta drives the formation of oxidative type IIX fibers in skeletal muscle. *Cell Metab* 5(1):35–46.
6. Narkar VA, et al. (2008) AMPK and PPARdelta agonists are exercise mimetics. *Cell* 134(3):405–415.
7. Hardie DG (2011) Energy sensing by the AMP-activated protein kinase and its effects on muscle metabolism. *Proc Nutr Soc* 70(1):92–99.
8. Gowans GJ, Hardie DG (2014) AMPK: A cellular energy sensor primarily regulated by AMP. *Biochem Soc Trans* 42(1):71–75.
9. Wu H, et al. (2002) Regulation of mitochondrial biogenesis in skeletal muscle by CaMK. *Science* 296(5566):349–352.
10. Naya FJ, et al. (2000) Stimulation of slow skeletal muscle fiber gene expression by calcineurin in vivo. *J Biol Chem* 275(7):4545–4548.
11. Kramerova I, et al. (2012) Impaired calcium calmodulin kinase signaling and muscle adaptation response in the absence of calpain 3. *Hum Mol Genet* 21(14):3193–3204.
12. Parsons SA, Wilkins BJ, Bueno OF, Molkentin JD (2003) Altered skeletal muscle phenotypes in calcineurin Aalpha and Abeta gene-targeted mice. *Mol Cell Biol* 23(12): 4331–4343.
13. Appleby MW, Ramsdell F (2003) A forward-genetic approach for analysis of the immune system. *Nat Rev Immunol* 3(6):463–471.
14. Park H, et al. (2012) Disruption of Fnip1 reveals a metabolic checkpoint controlling B lymphocyte development. *Immunity* 36(5):769–781.
15. Baba M, et al. (2006) Folliculin encoded by the BHD gene interacts with a binding protein, FNIP1, and AMPK, and is involved in AMPK and mTOR signaling. *Proc Natl Acad Sci USA* 103(42):15552–15557.
16. Hasumi H, et al. (2008) Identification and characterization of a novel folliculin-interacting protein FNIP2. *Gene* 415(1-2):60–67.
17. Takagi Y, et al. (2008) Interaction of folliculin (Birt-Hogg-Dubé gene product) with a novel Fnip1-like (FnipL/Fnip2) protein. *Oncogene* 27(40):5339–5347.
18. Linehan WM, et al. (2009) Hereditary kidney cancer: Unique opportunity for disease-based therapy. *Cancer* 115(10, Suppl):2252–2261.
19. Zong H, et al. (2002) AMP kinase is required for mitochondrial biogenesis in skeletal muscle in response to chronic energy deprivation. *Proc Natl Acad Sci USA* 99(25): 15983–15987.
20. Jäger S, Handschin C, St-Pierre J, Spiegelman BM (2007) AMP-activated protein kinase (AMPK) action in skeletal muscle via direct phosphorylation of PGC-1alpha. *Proc Natl Acad Sci USA* 104(29):12017–12022.
21. Laplante M, Sabatini DM (2012) mTOR signaling in growth control and disease. *Cell* 149(2):274–293.
22. Lin J, et al. (2004) Defects in adaptive energy metabolism with CNS-linked hyperactivity in PGC-1alpha null mice. *Cell* 119(1):121–135.
23. Ruegg UT (2013) Pharmacological prospects in the treatment of Duchenne muscular dystrophy. *Curr Opin Neurol* 26(5):577–584.
24. Koenig M, et al. (1987) Complete cloning of the Duchenne muscular dystrophy (DMD) cDNA and preliminary genomic organization of the DMD gene in normal and affected individuals. *Cell* 50(3):509–517.
25. Hoffman EP, Brown RH, Jr, Kunkel LM (1987) Dystrophin: The protein product of the Duchenne muscular dystrophy locus. *Cell* 51(6):919–928.
26. Monaco AP, et al. (1986) Isolation of candidate cDNAs for portions of the Duchenne muscular dystrophy gene. *Nature* 323(6089):646–650.
27. Bulfield G, Siller WG, Wight PA, Moore KJ (1984) X chromosome-linked muscular dystrophy (mdx) in the mouse. *Proc Natl Acad Sci USA* 81(4):1189–1192.
28. Im WB, et al. (1996) Differential expression of dystrophin isoforms in strains of mdx mice with different mutations. *Hum Mol Genet* 5(8):1149–1153.
29. Röckl KS, et al. (2007) Skeletal muscle adaptation to exercise training: AMP-activated protein kinase mediates muscle fiber type shift. *Diabetes* 56(8):2062–2069.
30. Garcia-Roves PM, Osler ME, Holmström MH, Zierath JR (2008) Gain-of-function R225Q mutation in AMP-activated protein kinase gamma3 subunit increases mitochondrial biogenesis in glycolytic skeletal muscle. *J Biol Chem* 283(51):35724–35734.
31. Mu J, Brozinick JT, Jr, Valladares O, Bucan M, Birnbaum MJ (2001) A role for AMP-activated protein kinase in contraction- and hypoxia-regulated glucose transport in skeletal muscle. *Mol Cell* 7(5):1085–1094.
32. Reznick RM, et al. (2007) Aging-associated reductions in AMP-activated protein kinase activity and mitochondrial biogenesis. *Cell Metab* 5(2):151–156.
33. Jørgensen SB, et al. (2007) Role of AMPKalpha2 in basal, training-, and AICAR-induced GLUT4, hexokinase II, and mitochondrial protein expression in mouse muscle. *Am J Physiol Endocrinol Metab* 292(1):E331–E339.
34. O'Neill HM, et al. (2011) AMP-activated protein kinase (AMPK) beta1beta2 muscle null mice reveal an essential role for AMPK in maintaining mitochondrial content and glucose uptake during exercise. *Proc Natl Acad Sci USA* 108(38):16092–16097.
35. Thomson DM, et al. (2007) Skeletal muscle and heart LKB1 deficiency causes decreased voluntary running and reduced muscle mitochondrial marker enzyme expression in mice. *Am J Physiol Endocrinol Metab* 292(1):E196–E202.
36. Rowe GC, Safdar A, Arany Z (2014) Running forward: New frontiers in endurance exercise biology. *Circulation* 129(7):798–810.
37. Hasumi H, et al. (2012) Regulation of mitochondrial oxidative metabolism by tumor suppressor FLCN. *J Natl Cancer Inst* 104(22):1750–1764.
38. Yan M, et al. (2014) The tumor suppressor folliculin regulates AMPK-dependent metabolic transformation. *J Clin Invest* 124(6):2640–2650.
39. Possik E, et al. (2014) Folliculin regulates ampk-dependent autophagy and metabolic stress survival. *PLoS Genet* 10(4):e1004273.
40. Park H, Tsang M, Iritani BM, Bevan MJ (2014) Metabolic regulator Fnip1 is crucial for iNKT lymphocyte development. *Proc Natl Acad Sci USA* 111(19):7066–7071.
41. Katsetos CD, Koutzaki S, Melvin JJ (2013) Mitochondrial dysfunction in neuromuscular disorders. *Semin Pediatr Neurol* 20(3):202–215.
42. Webster C, Silberstein L, Hays AP, Blau HM (1988) Fast muscle fibers are preferentially affected in Duchenne muscular dystrophy. *Cell* 52(4):503–513.
43. Handschin C, et al. (2007) PGC-1alpha regulates the neuromuscular junction program and ameliorates Duchenne muscular dystrophy. *Genes Dev* 21(7):770–783.
44. Chan MC, et al. (2014) Post-natal induction of PGC-1α protects against severe muscle dystrophy independently of utrophin. *Skelet Muscle* 4(1):2.